



## Synergistic Effects of Bacterial Nanocellulose and HUVEC-Conditioned Medium on Burn Wound Healing

Mohammad Valizadeh<sup>1</sup>, Rahim Hobbenaghi<sup>1</sup>✉, Rasoul Shahrooz<sup>2</sup>, Hassan Malekinejad<sup>3</sup>,  
Ali Karimi<sup>2</sup>, Hamed Valizadeh<sup>4</sup>

1. Department of Pathobiology, Faculty of Veterinary Medicine, Urmia University, Urmia, Iran
2. Department of Basic Sciences, Faculty of Veterinary Medicine, Urmia University, Urmia, Iran
3. Department of Pharmacology and Toxicology, School of Pharmacy, Urmia University of Medical Sciences, Urmia, Iran
4. Tuberculosis and Lung Disease Research Center, Tabriz University of Medical Sciences, Tabriz, Iran

### Article Info

#### Article Type:

Original Article

#### Article history:

Received

15 Sep 2025

Received in revised form

03 Feb 2026

Accepted

09 Feb 2026

Published online

10 Mar 2026

#### Publisher

Fasa University of  
Medical Sciences

### Abstract

**Background & Objective:** Burn injuries are inherently challenging to manage due to extensive tissue destruction and the substantial edema that ensues. This experimental animal study aimed to evaluate the synergistic effects of bacterial nanocellulose (BC) dressing combined with human umbilical vein endothelial cell-conditioned medium (HUVEC-CM) on the healing process of second-degree burn wounds in rats.

**Materials & Methods:** Fifty male Wistar rats were randomly allocated into five groups: healthy control (no wound), negative control (untreated wounds, sham), BC dressing treatment, HUVEC-CM treatment, and combined BC plus HUVEC-CM treatment (n = 10 per group). A standardized burn wound with a diameter of 10 mm was created on the dorsal surface of each rat. The healing process was assessed macroscopically, using wound contraction percentage, and histopathologically over a 14-day period.

**Results:** The combination group demonstrated the smallest wound area by day 3 and exhibited significantly enhanced wound closure on days 7 and 14 (p < 0.05). On day 3, wound closure percentages were as follows: negative control (-1.8 ± 1.7%), BC group (5.6 ± 2.1%), HUVEC-CM group (4.9 ± 2.4%), and combination group (9.1 ± 6.3%). The greatest degree of wound closure was observed in the combination group on day 14 (71.3 ± 6.8%). Histological analysis revealed that the combination treatment reduced early necrosis and inflammation, promoted granulation tissue formation and angiogenesis by day 7, and resulted in complete re-epithelialization by day 14.

**Conclusion:** The combined application of BC and HUVEC-CM synergistically enhances burn wound healing by mitigating early tissue damage and promoting subsequent regenerative processes. This approach represents a promising bioactive strategy for advanced burn wound management.

**Keywords:** Burns; Wound; Healing; Rats; Tissue Engineering

**Cite this article:** Valizadeh M, Hobbenaghi R, Shahrooz R, Malekinejad H, Karimi A, Valizadeh H. Synergistic Effects of Bacterial Nanocellulose and HUVEC-Conditioned Medium on Burn Wound Healing. *J Adv Biomed Sci.* 2026; 16(2): 167-178.

**DOI:** 10.18502/jabs.v16i2.20878

### Introduction

Burn injuries constitute a major global health

✉ **Corresponding Author:** Rahim Hobbenaghi,  
Department of Pathobiology, Faculty of Veterinary  
Medicine, Urmia University, Urmia, Iran.

**Email:** r.hobbenaghi@urmia.ac.ir

concern, causing substantial tissue damage in millions of individuals each year and often leading to long-term disability or mortality (1). These injuries initiate a systemic inflammatory response that can result in local ischemia and increased susceptibility to infection (2).





Valizadeh M, et al.

Partial-thickness, or second-degree, burn wounds extend into both the epidermis and dermis and are typically characterized by marked hypersensitivity and pain (3).

The tissue surrounding the burn site, referred to as the zone of stasis, remains particularly vulnerable. Although this region is initially viable, it is at significant risk of progressing to necrosis within 48 to 72 hours post-injury due to compromised blood flow and persistent inflammation (4,5). Consequently, a primary objective in burn management is the preservation of the zone of stasis and the prevention of further tissue deterioration (4).

An effective wound dressing should fulfill several critical functions, including preventing infection, maintaining a moist environment, managing exudate, and promoting tissue repair. In this context, biomaterials have attracted considerable attention in advanced wound care. Bacterial nanocellulose (BC) has emerged as a promising candidate for burn treatment owing to its excellent biocompatibility, high purity, and nanofibrillar architecture, which closely resembles the natural extracellular matrix (ECM) (6–8). BC exhibits a high capacity for fluid absorption and retention, forms a protective barrier against microbial invasion, and possesses favorable mechanical properties, making it particularly suitable for wound protection (6,8). Moreover, its porous structure facilitates gas exchange and supports cellular adhesion and migration (8,9). Recent studies have demonstrated the efficacy of BC-based dressings in enhancing re-epithelialization and reducing infection rates in burn models (8,10).

Wound healing is a complex, multistage process encompassing hemostasis, inflammation, tissue regeneration, and remodeling. The regenerative phase involves granulation tissue formation, angiogenesis, and re-epithelialization, all of which depend on key growth factors such as vascular endothelial growth factor (VEGF), basic fibroblast growth

factor (bFGF), and transforming growth factor-beta (TGF- $\beta$ ) (11). Therapeutic strategies targeting these molecular mediators have shown considerable promise.

Human umbilical vein endothelial cells (HUVECs) secrete a wide array of bioactive molecules, including VEGF, bFGF, and angiopoietins, which play critical roles in angiogenesis, modulation of inflammation, and tissue regeneration (12,13). The conditioned medium derived from these cells (HUVEC-CM) contains a rich repertoire of therapeutic factors and represents a cell-free approach to promoting tissue repair (14,15). The application of endothelial cell-derived conditioned media has been shown to enhance angiogenesis and accelerate wound closure, particularly in models of impaired healing (16).

Despite these advantages, a major limitation of topical CM therapy is the rapid clearance of soluble factors from the wound site, which reduces their local bioavailability and therapeutic efficacy. Although both BC, as a structural scaffold, and HUVEC-CM, as a source of bioactive molecules, have individually demonstrated therapeutic potential, their combined application, particularly in the context of burn wounds, remains insufficiently explored.

We hypothesize that incorporating HUVEC-CM into a BC-based hydrogel may yield a synergistic bioactive dressing by enhancing the local retention and sustained release of therapeutic factors. In this configuration, the BC matrix is expected to function as a controlled delivery platform, prolonging the availability of growth factors while simultaneously providing structural support and maintaining an optimal moist environment. Such an integrated approach is designed to address both the immediate needs of burn wounds, including barrier protection and inflammation control, and the subsequent regenerative processes, such as angiogenesis, granulation tissue formation, and re-epithelialization.



Accordingly, the present study was designed to evaluate the synergistic effects of a BC-based dressing impregnated with HUVEC-CM on the healing of second-degree burn wounds in a rat model.

## Materials and Methods

### Ethical Statement

The animal study protocol was approved by the Animal Ethics Committee of the Faculty of Veterinary Medicine, Urmia University (Approval Code: IR-UU-AEC-3/84; Date: 18/11/2025). All experimental procedures were conducted in strict accordance with institutional guidelines for the care and use of laboratory animals. Every effort was made to minimize animal suffering and to reduce the number of animals used.

### Animals and Experimental Design

A total of fifty male Wistar rats (approximately eight weeks old; body weight  $150 \pm 20$  g) were obtained from the Animal Breeding Center of Urmia University of Medical Sciences. The animals were housed individually in standard cages under controlled environmental conditions ( $23 \pm 2^\circ\text{C}$ ; 12-hour light/dark cycle) with ad libitum access to food and water. The rats were randomly allocated into five experimental groups ( $n = 10$  per group) using a computer-generated randomization sequence. The sample size was determined based on previously published studies employing comparable burn wound models in rodents (17).

The experimental groups were defined as follows:

1. **Healthy Control:** No wound induction.
2. **Negative Control:** Burn wound without any treatment
3. **BC Group:** Burn wound covered with sterile BC hydrogel (2 x 2 cm, 2 mm thickness). The smooth surface (formerly in contact with the culture medium) was placed directly onto the wound bed

4. **HUVEC-CM Group:** Burn wound treated with topical application of 100  $\mu\text{L}$  of reconstituted HUVEC-CM solution (containing approximately 350 ng of the lyophilized CM powder, based on the preparation protocol).

5. **Combination Group:** Burn wound treated with BC hydrogel impregnated with HUVEC-CM. Sterile BC films were impregnated under aseptic conditions with 100  $\mu\text{L}$  of the reconstituted HUVEC-CM solution (approximately 350 ng lyophilized powder), allowed to dry, and then applied to the wound with the smooth surface in direct contact with the wound bed.

### Preparation of Bacterial Nanocellulose Film

BC was produced using *Komagataeibacter xylinus* PTCC 1734 cultured in a sucrose-based liquid medium supplemented with yeast extract and peptone. Cultures were incubated under static conditions at  $30^\circ\text{C}$  for 7 days. The resulting BC pellicles were purified by treatment with 1% (w/v) NaOH at  $80^\circ\text{C}$  for 1 hour to remove bacterial cells and residual medium components, followed by extensive washing with distilled water until a neutral pH was achieved. The purified BC was subsequently homogenized, cast into films, and dried in an incubator at  $40^\circ\text{C}$ . The dried films were sterilized by autoclaving at  $121^\circ\text{C}$  for 15 minutes prior to use as wound dressings (8,18). The BC material was provided by Fanavaran Nanozist Company (Urmia University Technology Park, Urmia, Iran). The biosynthesis and characterization procedures were consistent with the established static cultivation method described by Ghorbani et al. (2022) (8). For application, the smooth surface of the film, corresponding to the side previously in contact with the culture medium, was positioned directly against the wound bed.

### Preparation of HUVEC Conditioned Media

HUVECs; ATCC PCS-100-013, passage 3 were cultured in endothelial cell growth medium-2 under standard conditions.



Valizadeh M, et al.

Upon reaching 80–90% confluence, the cells were thoroughly rinsed to remove residual growth medium and subsequently incubated in serum-free DMEM (Biosera, LM-1101) for 48 hours. The conditioned medium was then collected, centrifuged at  $3000 \times g$  for 10 minutes to remove cellular debris, and filtered through a  $0.22 \mu\text{m}$  membrane filter. The filtrate was concentrated 50-fold via freeze-drying and stored at  $-80^\circ\text{C}$  until use.

For in vivo application, the lyophilized HUVEC-CM powder was reconstituted in sterile distilled water. A volume of  $100 \mu\text{L}$ , containing approximately 350 ng of lyophilized material, was applied per wound either directly (HUVEC-CM group) or used for BC impregnation (Combination group) (14).

### **Burn Wound Model**

Second-degree burn wounds were induced using a custom-fabricated brass rod (10 mm diameter; 100 g). The rod was heated in boiling water to  $100^\circ\text{C}$ , with the temperature verified using a calibrated thermometer. Under general anesthesia induced by ketamine (100 mg/kg; Bioveta, Czech Republic) and xylazine (10 mg/kg; Bioveta, Czech Republic), the dorsal skin of each rat was shaved and disinfected. The heated rod was then applied vertically to the skin under its own weight for 10 seconds, ensuring consistent pressure and contact. This procedure produced a standardized partial-thickness burn wound with a diameter of 10 mm (3,19).

### **Wound Healing planimetry**

#### **Macroscopic Evaluation**

Wound areas were measured on days 0, 3, 7, and 14 post-burn using a digital caliper. Two perpendicular diameters (longest and shortest) were measured for each wound, and the wound area was calculated using the formula for an ellipse:  $\text{Area} = \pi \times (d1/2) \times (d2/2)$ . The percentage of wound contraction for each time point (X) was calculated using the formula:  $[(\text{Initial Area on Day 0} - \text{Open Area on Day X}) / \text{Initial Area on Day 0}] \times 100$  (3)

At each pre-determined endpoint (days 3, 7, and 14), wound dimensions were measured by a blinded investigator just before the animals were euthanized for tissue collection.

### **Histopathological Analyse**

Tissue samples were fixed in 10% buffered formalin, followed by routine histological processing, paraffin embedding, and sectioning. Sections of  $5 \mu\text{m}$  thickness were stained with hematoxylin and eosin (H&E) for general morphological evaluation. To assess collagen deposition and organization, adjacent sections were stained using Van Gieson's method. Histopathological evaluation was conducted using a comparative descriptive approach across experimental groups. All assessments and scoring procedures were performed by an experienced pathologist blinded to group allocation.

### **Chemical Analysis (FTIR)**

The chemical structure and surface functional groups of the BC film were analyzed using Fourier-Transform Infrared (FTIR) spectroscopy. The analysis was performed on a Jasco FT/IR-4100 spectrometer in the wavenumber range of  $4000$  to  $450 \text{ cm}^{-1}$ . Spectra were acquired to confirm the chemical identity of cellulose and to verify the efficacy of the purification process by ensuring the absence of characteristic peaks from proteins or other medium contaminants (8).

### **Field Emission Scanning Electron Microscopy (FESEM)**

The surface morphology of BC films following impregnation with HUVEC-CM and subsequent drying, representing the final dressing used in the Combination group, was examined using field emission scanning electron microscopy (FESEM). Imaging was performed using a TESCAN MIRA3-FEG microscope (TESCAN, Czech Republic) at Tabriz University. This analysis enabled detailed visualization of the microstructure and confirmed the preservation of the nanofibrous architecture after impregnation.

## Statistical Analysis

Data are presented as mean  $\pm$  standard deviation (SD). All statistical analyses were conducted using SPSS software (version 26.0; IBM Corp., Armonk, NY, USA). The normality of data distribution was assessed using the Shapiro–Wilk test. For comparisons of wound closure percentages and other quantitative variables among the five groups at each time point, one-way analysis of variance (ANOVA) was employed. When a statistically significant difference was detected, post hoc pairwise comparisons were performed using Tukey’s honestly significant difference (HSD) test. A  $P$ -value  $< 0.05$  was considered statistically significant. In addition to  $P$ -values, effect sizes (partial eta squared,  $\eta^2$ ) are reported for significant ANOVA results in order to quantify the magnitude of the observed differences.

## Results

### Material Characterization

The characterization of the synthesized

BC film, based on Ghorbani et al. (2022), together with that of the final composite dressing, confirmed its suitability for wound healing applications. Field emission scanning electron microscopy (FESEM) of the BC film following impregnation with HUVEC-CM and subsequent drying revealed a well-preserved, highly porous, three-dimensional nanofibrous network composed of interconnected fibrils. Notably, this microarchitecture closely resembles key structural features of the native ECM, thereby facilitating cell adhesion, proliferation, and gas exchange. Furthermore, FESEM analysis of the final BC–HUVEC-CM composite dressing confirmed that the nanofibrous architecture remained intact after impregnation (Figure 1).

### Fourier-Transform Infrared Spectroscopy

FTIR spectroscopy verified the chemical purity of the BC, demonstrating characteristic cellulose peaks corresponding to O–H, C–H, and C–O–C stretching vibrations, with no detectable peaks attributable to proteins or other contaminants.

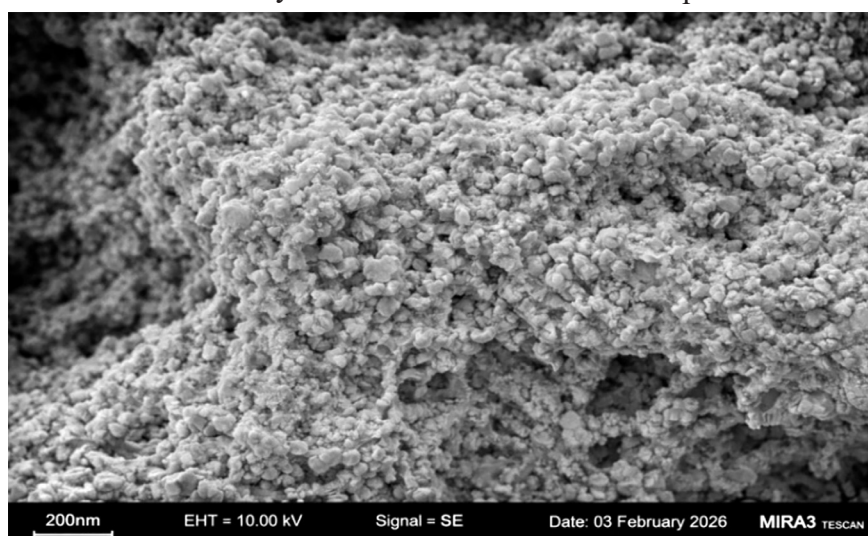


**Figure 1.** Field Emission Scanning Electron Microscopy (FESEM) representation of the Bacterial Nanocellulose (BC) dressing after impregnation with HUVEC-CM and drying. The Figure demonstrates the preservation of the highly porous, three-dimensional nanofibrous network characteristic of BC following the loading process. Granular and particulate deposits on the nanofibrils are suggestive of surface deposition of CM-derived components from the HUVEC-CM. The interconnected fibrillar structure, with fibril diameters typically below 100 nm, is maintained, which is essential for mimicking the extracellular matrix (ECM), facilitating gas exchange, and providing a scaffold for cell migration and attachment during wound healing.

\*Imaging parameters: Accelerating voltage = 10.00 kV, Detector = Secondary Electron (SE)

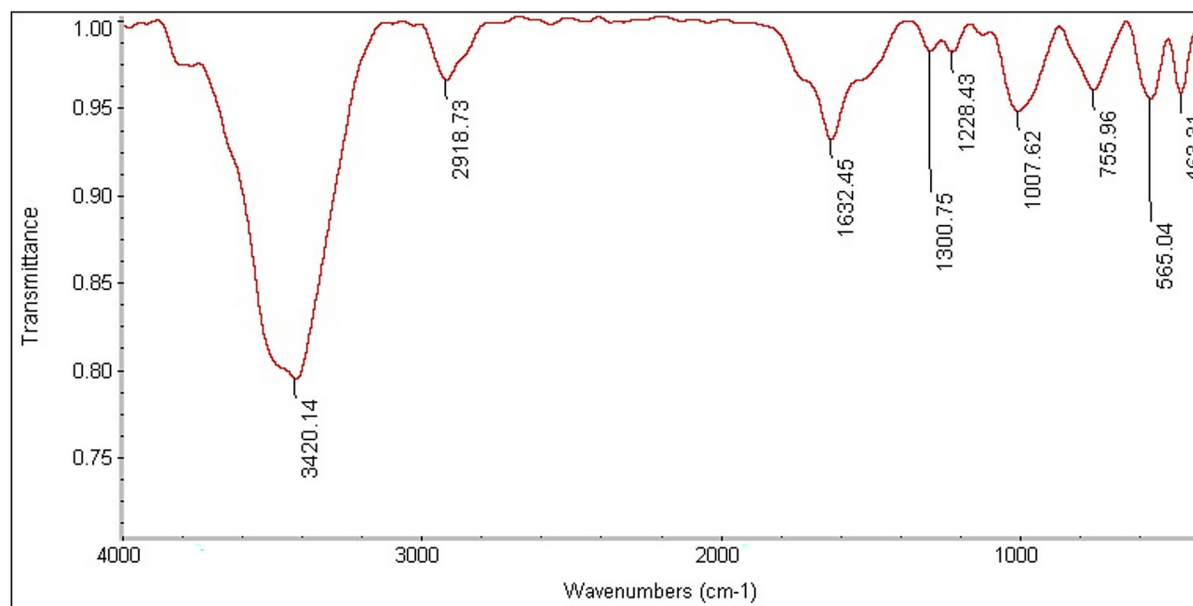


**Figure 2.** FTIR spectrum of the synthesized bacterial nanocellulose (BC) film.

The spectrum shows characteristic peaks of cellulose: a broad O–H stretching band at ~3400–3200  $\text{cm}^{-1}$ , C–H stretching at ~2900  $\text{cm}^{-1}$ , and strong C–O–C/C–O stretching vibrations between 1200–1000  $\text{cm}^{-1}$ . The absence of peaks indicative of protein contaminants confirms the efficacy of the purification process and the chemical purity of the BC material

**Table 1.** Wound Closure Percentage during the Healing Process (Mean  $\pm$  SD)

Group	Day 3	Day 7	Day 14
Sham	-1.8 $\pm$ 1.7 a	12.3 $\pm$ 9.4 a	36.5 $\pm$ 11.2 a
BC Group	5.6 $\pm$ 2.1 b	26.5 $\pm$ 7.8 b	58.9 $\pm$ 8.5 b
HUVEC-CM Group	4.9 $\pm$ 2.4 b	24.1 $\pm$ 8.3 b	55.8 $\pm$ 9.1 b
Combination Group	9.1 $\pm$ 6.3 c	34.1 $\pm$ 7.2 c	71.3 $\pm$ 6.8 c

These findings confirm the effectiveness of the purification process (8). The FTIR analysis was independently repeated in the present study and yielded highly consistent results, with clearly defined peaks as illustrated in Figure 2.

### Macroscopic Wound Healing

Wound closure was quantitatively assessed throughout the healing period (Table 1). On day 3, the wound area in the negative control group exceeded that of all treatment groups. The negative wound closure percentage observed in the sham group reflects an increase in wound area, attributable to inflammation and early necrotic progression. In contrast, all treatment groups exhibited reduced wound areas, with the combination group demonstrating the most pronounced improvement ( $P < 0.05$ ). Notably, this group displayed the smallest wound area

as early as day 3 and achieved significantly greater wound closure on days 7 and 14 compared with all other treated groups ( $P < 0.05$ ;  $\eta^2 = 0.45$ ), indicating a large effect size (Table 1). Wound closure data are presented as mean  $\pm$  SD. Within each time point, different superscript letters (a, b, c) denote statistically significant differences ( $P < 0.05$ ; one-way ANOVA followed by Tukey's test). The overall ANOVA for day 14 demonstrated a large effect size ( $\eta^2 = 0.45$ ). A negative wound closure percentage indicates an increase in wound area relative to baseline (day 0).

### Histopathological Findings

Key qualitative histopathological findings are summarized in Table 2 and described below. The analysis was performed by a pathologist blinded to group allocation.



**Table 2.** Summary of Key Histopathological findings at Different Time Points.

Parameter	Group	Day 3	Day 7	Day 14
Necrosis Extension	Sham	+++	++	+
	BC	++	+	-
	HUVEC-CM	+	+	-
	Combination	+	-	-
Inflammatory Cell Infiltrate	Sham	+++ (Mainly PMNs)	+++ (PMNs & Macrophages)	++ (Macrophages & Lymphocytes)
	BC	++	++	+
	HUVEC-CM	++	+	+
	Combination	+	+	±
Granulation Tissue Formation	Sham	-	+	++
	BC	-	++	+++
	HUVEC-CM	±	++	+++
	Combination	+	+++	+++
Angiogenesis	Sham	-	+	++
	BC	-	++	++
	HUVEC-CM	+	+++	+++
	Combination	+	+++	+++
Epithelialization	Sham	-	±	+
	BC	-	+	++
	HUVEC-CM	-	+	++
	Combination	-	++	+++

Table 2 summarizes what was seen under the microscope (histopathology) at different points in time.

The symbols mean:

\* +++: A lot/Very Common \* ++: Moderate amount \* +: Small amount/Somewhat Common \* ±: Very Little/Just Starting

-: Not Present PMNs stands for Polymorphonuclear Neutrophils, which are a type of white blood cell involved in inflammation.

### Day 3 Post-Burning:

**Negative Control:** Extensive epidermal and dermal damage was observed, accompanied by marked hyperemia, neutrophil-dominated inflammation, and pronounced edema beneath the burned epidermis.

**BC Group:** Epidermal damage was present but remained relatively superficial. Inflammatory infiltration was reduced compared with the negative control. Although edema persisted, no evidence of granulation tissue formation or angiogenesis was detected.

**HUVEC-CM Group:** Inflammatory cell infiltration was lower than in the negative control group. Macrophages and a limited number of fibroblasts were observed within the wound bed, and edema was comparatively mild.

**Combination Group:** This group

exhibited the least degree of tissue damage and inflammation, characterized by reduced neutrophil infiltration, increased macrophage presence, active fibroblast proliferation, early neovascularization (capillary structures with discernible lumina), and only minimal edema.

### Day 7 Post-Wounding:

**Negative Control:** Persistent and pronounced inflammation was evident. Granulation tissue formation was limited, with sparse neovascularization and minimal re-epithelialization (Figure 3).

**BC Group:** Epidermal regeneration was evident at the wound margins. Granulation tissue had developed, accompanied by detectable eosinophilic extracellular matrix deposition. Inflammatory infiltration was reduced relative to day 3.

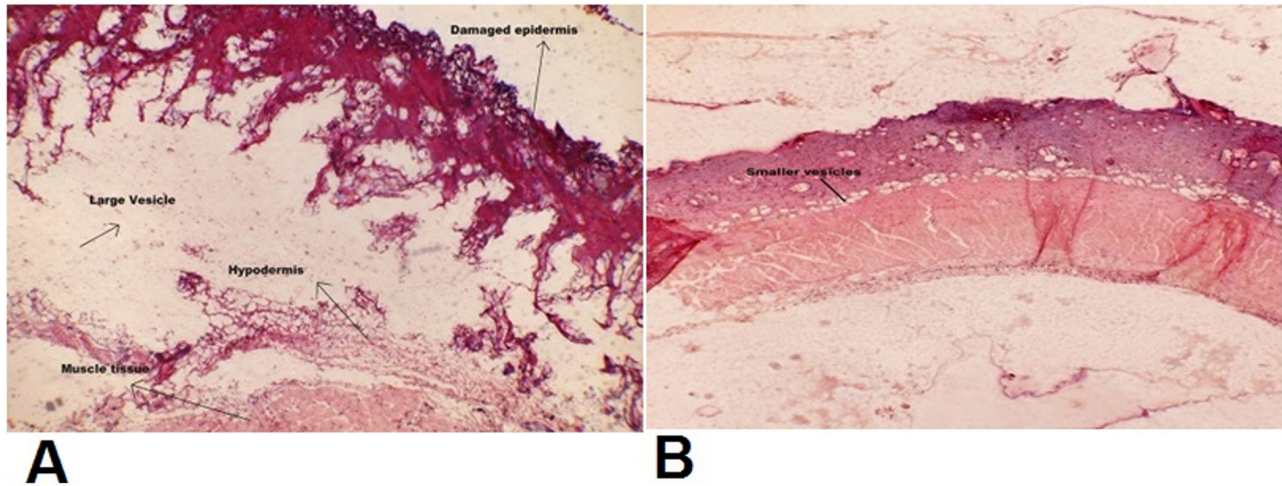


**Figure 3.** Second-Degree burned tissue healing on day 7, 40X, H& E staining. **A)** sham group: large vesicle has formed beneath the necrotic and burned epidermis. **B)** Combination group: The formed vesicles are very limited and small

**HUVEC-CM Group:** Compared with the BC group, this group exhibited increased neovascularization, enhanced fibroblast proliferation, and more extensive granulation tissue formation.

**Combination Group:** Granulation tissue was well developed, displaying increased vascular density and prominent eosinophilic matrix deposition consistent with collagen accumulation. Tissue regeneration was more advanced, inflammation was further attenuated,

and epidermal expansion exceeded that observed in all other treatment groups. Findings from Van Gieson staining corroborated the presence of more abundant and better-organized collagen fibers in this group (Figure 3).

**Day 14 Post-Wounding:**

**Negative Control:** Re-epithelialization remained incomplete, with limited and disorganized granulation tissue. Inflammatory cells, particularly neutrophils, persisted within the wound area (Figure 4).

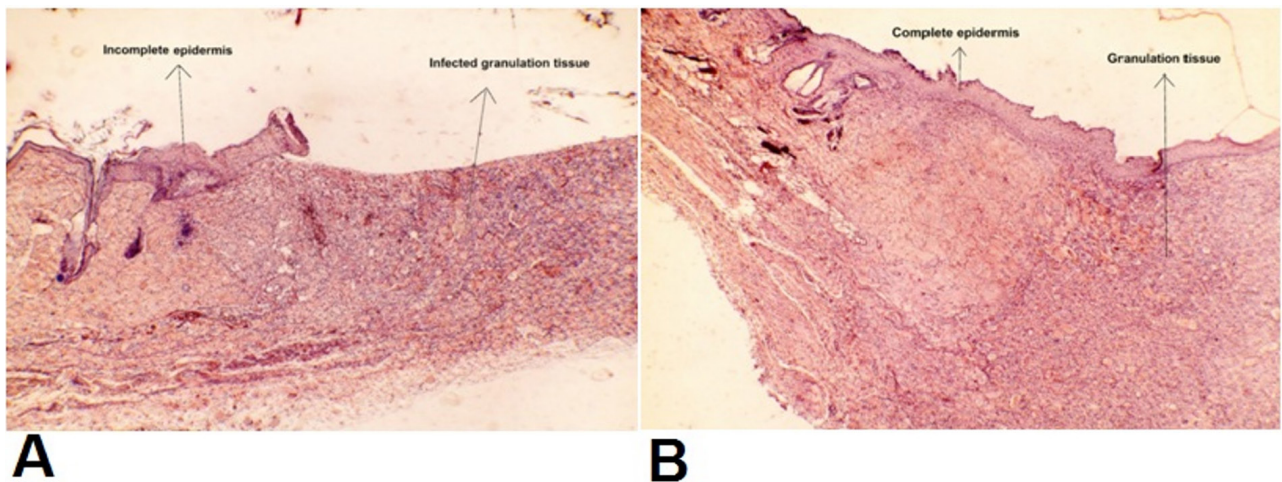


**Figure 4.** Second-degree burn healing on day ,14, 40X magnification; H&E staining. **A)** sham group: The newly formed epidermis incompletely covers the wound surface, and the wound area remains open. Large number of inflammatory cells, predominantly neutrophils, infiltrated in the dermis and hypodermis, forming a subcutaneous abscess. **B)** combination group: The epidermis completely covers the wound surface. Granulation tissue has formed in an organized manner at the wound site, and the infiltration of inflammatory cells is significantly less



**BC & HUVEC-CM Groups:** Near-complete epidermal coverage was observed, accompanied by extensive granulation tissue formation and improved structural organization, including collagen deposition.

**Combination Group:** Near-complete re-epithelialization was achieved, with advanced tissue architecture and more orderly, well-organized collagen fibers. Inflammatory cell infiltration was markedly reduced. These observations, although qualitative in nature, consistently indicate enhanced tissue maturation in this group and should be interpreted within the context of descriptive histological analysis (Figure 4).

## Discussion

The present study demonstrates that a BC dressing combined with HUVEC-CM synergistically accelerates the healing of second-degree burn wounds in a rat model. Notably, the combined treatment exerted beneficial effects across all phases of wound healing, ranging from the initial inflammatory response to subsequent tissue remodeling.

Burn injuries are known to exacerbate damage within the surrounding zone of stasis due to impaired perfusion and sustained inflammation, often culminating in secondary necrosis. In this context, our findings indicate that the BC plus HUVEC-CM dressing effectively limited secondary tissue damage as early as day 3. This early protective effect is most plausibly attributable to the integrated physical and bioactive properties of the composite dressing. Specifically, the BC matrix, characterized by its highly porous and nanofibrous architecture (8), provides an immediate physical barrier against microbial invasion while simultaneously maintaining a moist microenvironment that is essential for cellular viability and migration (6,7). Concurrently, HUVEC-CM, enriched with angiogenic and anti-inflammatory mediators, likely attenuates the initial inflammatory

cascade (20).

Of particular importance is the observed shift in the inflammatory cell profile within the combination group, characterized by reduced neutrophil infiltration alongside increased macrophage presence. This pattern suggests an accelerated transition from the pro-inflammatory phase to the proliferative phase of healing. Given the pivotal role of macrophages in orchestrating tissue repair through the secretion of growth factors and cytokines that both suppress inflammation and promote regeneration, this shift represents a critical mechanistic insight (21).

During the proliferative phase, spanning days 7 to 14, the combination treatment yielded markedly superior outcomes in terms of granulation tissue formation, angiogenesis, and re-epithelialization. This enhanced regenerative response is likely driven by a synergistic interplay between structural and biochemical cues. The BC scaffold, by closely mimicking the native ECM (8), provides a three-dimensional framework conducive to the infiltration, adhesion, and proliferation of fibroblasts, keratinocytes, and endothelial cells (9,10). Simultaneously, HUVEC-CM, retained within this matrix, appears to function as a localized reservoir of bioactive factors, thereby enhancing their persistence at the wound site.

Angiogenic mediators such as VEGF and basic fibroblast growth factor (bFGF), known constituents of HUVEC-CM (11,13), likely contribute to the robust neovascularization observed, which is essential for the delivery of oxygen and nutrients to regenerating tissues (22). In parallel, transforming growth factor-beta (TGF- $\beta$ ) may facilitate fibroblast differentiation into myofibroblasts and promote ECM deposition, thereby advancing tissue maturation (11,23).

Collectively, these findings are consistent with, and extend, existing literature. While previous studies have established the efficacy



Valizadeh M, et al.

of BC-based dressings in wound management (10,24) and demonstrated the pro-angiogenic potential of endothelial cell-derived conditioned media (16,25), investigations into their combined application, particularly in burn wound models, remain limited. The present study provides compelling evidence that their integration yields a synergistic effect, producing significantly improved healing outcomes compared with either modality alone. This synergy is most plausibly explained by the convergence of structural support and the sustained, localized delivery of biochemical signals.

### Conclusion

In summary, the findings of this study demonstrate that a composite dressing comprising BC and human umbilical vein HUVEC-CM synergistically enhances the healing of second-degree burn wounds in a rat model. The BC scaffold provides essential structural support and barrier protection, whereas HUVEC-CM supplies a rich repertoire of bioactive factors that modulate the wound healing cascade. Together, these components appear to operate through a dual mechanism: first, by mitigating early-stage tissue damage, inflammation, and edema; and second, by actively promoting the proliferative phase, as evidenced by enhanced granulation tissue formation, angiogenesis, and re-epithelialization. The observed synergy further suggests that the BC matrix may function as an effective carrier or reservoir for CM-derived factors, thereby improving their local retention and bioavailability. Despite these promising findings, the precise mechanistic basis of this interaction, particularly with respect to release kinetics and factor stability, warrants further investigation. Future studies employing more complex experimental models and, ultimately, clinical trials will be essential to facilitate the translation of this combinatorial strategy into clinical practice.

### **Strengths, Limitations, and Future Directions**

**Strengths:** A principal strength of this study lies in the introduction of a novel combinatorial therapeutic strategy that integrates a well-characterized BC biomaterial with a cell-free, bioactive conditioned medium. Moreover, the study design incorporates a comprehensive in vivo evaluation over a 14-day period, combining quantitative macroscopic assessments with detailed histopathological analyses, thereby providing robust evidence of a synergistic healing effect.

**Limitations:** Several limitations warrant consideration. First, the use of a healthy, young rat model does not fully recapitulate the impaired healing conditions observed in clinical populations, such as individuals with diabetes or immunodeficiency. Second, although histopathological analysis offers valuable qualitative insights, it remains inherently descriptive. Future investigations would benefit from incorporating quantitative methodologies, such as immunohistochemical analysis of specific cellular markers and biochemical assays, including hydroxyproline quantification for collagen content. Furthermore, the proposed mechanism of action, wherein BC functions as a sustained-release platform for bioactive factors, remains hypothetical in the absence of supporting in vitro release kinetics data. Finally, although the sample size was sufficient to detect statistically significant differences in primary outcomes, larger cohorts would enhance statistical power and enable more refined subgroup analyses.

**Future Directions:** Building on these findings, future research should focus on: 1) elucidating the precise molecular mechanisms of the synergy through in vitro co-culture studies and release kinetics studies to validate the proposed sustained-release profile, 2) evaluating the dressing in chronified or comorbid wound models, and 3) exploring the



controlled release kinetics of growth factors from the BC matrix to optimize the delivery profile.

### Acknowledgements

The authors gratefully acknowledge the support of the University Research Vice-Chancellor and colleagues for their assistance in conducting this study. The authors also acknowledge the use of language editing tools to enhance the clarity and readability of the manuscript.

### Conflict of Interest

The authors declare no conflict of interest related to this article.

### Funding

This research received no specific grant from any funding agency in the public, commercial, or not-for-profit sectors. The study was conducted as part of an academic thesis project (code no. 29361), and all associated costs were covered by institutional resources.

### Ethical Considerations

All procedures involving animals were conducted in accordance with institutional ethical standards and national guidelines for the care and use of laboratory animals. The study protocol was approved by the Animal Ethics Committee of the Faculty of Veterinary Medicine, Urmia University (Approval Code: IR-UU-AEC-3/84; Date: 18/11/2025). Every effort was made to minimize animal suffering and to reduce the number of animals used, in accordance with the principles of Replacement, Reduction, and Refinement.

### Code of Ethics

This study was conducted as part of an academic thesis at the Faculty of Veterinary Medicine, Urmia University, in full compliance

with institutional and national ethical guidelines for animal research. The ethics approval code is IR-UU-AEC-3/84, and the thesis registration number is 29361. The authors affirm that no fabrication, falsification, or inappropriate data manipulation occurred during the course of this research. No human subjects were involved.

### Author Contributions

M. Valizadeh and R. Hobbenaghi conceived and designed the study. M. Valizadeh, A. Karimi, and H. Valizadeh conducted the experiments and collected the data. R. Hobbenaghi, R. Shahrooz, and H. Malekinejad supervised the study and provided essential resources. M. Valizadeh drafted the manuscript. R. Hobbenaghi, R. Shahrooz, and H. Malekinejad critically revised the manuscript for important intellectual content. All authors reviewed and approved the final version of the manuscript.

### References

- 1 Haruta A, Mandell SP. Assessment and Management of Acute Burn Injuries. *Phys Med Rehabil Clin N Am.* 2023;34(4):795-811.
- 2 Rowan MP, Cancio LC, Elster EA, Burmeister DM, Rose LF, Natesan S, et al. Burn wound healing and treatment: review and advancements. *Crit Care.* 2015;19:243.
- 3 Pereira DST, Lima-Ribeiro MHM, Pontes-Filho NT, Carneiro-Leão AMA, Correia MTDS. Development of Animal Model for Studying Deep Second-Degree Thermal Burns. *J Biomed Biotechnol.* 2012;460841.
- 4 Jeschke MG, van Baar ME, Choudhry MA, Chung KK, Gibran NS, Logsetty S. Burn injury. *Nat Rev Dis Primers.* 2020;6(1):11.
- 5 Kim H, Shin S, Han D. Review of history of basic principles of burn wound management. *Medicina.* 2022;58(3):400.
- 6 Fu L, Zhang J, Yang G. Present status and applications of bacterial cellulose-based materials for skin tissue repair. *Carbohydr Polym.* 2013;92(2):1432-42.
- 7 Portela R, Leal CR, Almeida PL, Sobral RG. Bacterial cellulose: a versatile biopolymer for wound dressing applications. *Microb Biotechnol.* 2019;12(4):586-610.
- 8 Ghorbani M, Tajik H, Moradi M, Molaei R, Alizadeh A. One-pot microbial approach to synthesize



Valizadeh M, et al.

- carbon dots from baker's yeast-derived compounds for the preparation of antimicrobial membrane. *J Environ Chem Eng.* 2022;10(3):107525.
- 9 Wang J, Tavakoli J, Tang Y. Bacterial cellulose production, properties and applications with different culture methods - A review. *Carbohydr Polym.* 2019;219:63-76.
  - 10 Mohamad N, Loh EYX, Fauzi MB, Ng MH, Mohd Amin MCI. In vivo evaluation of bacterial cellulose/ acrylic acid wound dressing hydrogel containing keratinocytes and fibroblasts for burn wounds. *Drug Deliv Transl Res.* 2019;9(2):444-52.
  - 11 Barrientos S, Brem H, Stojadinovic O, Tomic-Canic M. Clinical application of growth factors and cytokines in wound healing. *Wound Repair Regen.* 2014;22(5):585-601.
  - 12 Liu J, Yan Z, Yang F, Huang Y, Yu Y, Zhou L, et al. Exosomes Derived from Human Umbilical Cord Mesenchymal Stem Cells Accelerate Cutaneous Wound Healing by Enhancing Angiogenesis through Delivering Angiopoietin-2. *Stem Cell Rev Rep.* 2021;17(2):305-17.
  - 13 Johnson KE, Wilgus TA. Vascular Endothelial Growth Factor and Angiogenesis in the Regulation of Cutaneous Wound Repair. *Adv Wound Care (New Rochelle).* 2014;3(10):647-61.
  - 14 Pawitan JA. Prospect of stem cell conditioned medium in regenerative medicine. *Biomed Res Int.* 2014;965849.
  - 15 Teng L, Maqsood M, Zhu M, Zhou Y, Kang M, Zhou J, et al. Exosomes Derived from Human Umbilical Cord Mesenchymal Stem Cells Accelerate Diabetic Wound Healing via Promoting M2 Macrophage Polarization, Angiogenesis, and Collagen Deposition. *Stem Cell Rev Rep.* 2022;18(7):2445-60.
  - 16 Kim JY, Song SH, Kim KL, Ko JJ, Im JE, Yie SW, et al. Human cord blood-derived endothelial progenitor cells and their conditioned media exhibit therapeutic equivalence for diabetic wound healing. *Cell Transplant.* 2010;19(12):1635-44.
  - 17 Cai EZ, Ang CH, Raju A, Tan KB, Hing ECH, Loo Y, Lim TC. Creation of consistent burn wounds: a rat model. *Arch Plast Surg.* 2014;41(4):317-24.
  - 18 Shiravani Z, Aliakbarlu J, Moradi M. Application of bacterial nanocellulose film loaded with sodium nitrite, sumac, and black carrot extracts to reduce sodium nitrite, extend shelf life, and inhibit *Clostridium perfringens* in cooked beef ham. *Food Sci Technol.* 2023;45(3):112-25. [In Persian]
  - 19 Regas FC, Ehrlich HP. Elucidating the vascular response to burns with a new rat model. *J Trauma.* 1992;32(5):557-63.
  - 20 Rautiainen S, Laaksonen T, Koivuniemi R. Angiogenic effects and crosstalk of adipose-derived mesenchymal stem/stromal cells and their extracellular vesicles with endothelial cells. *Int J Mol Sci.* 2021;22(19):10890
  - 21 Koh TJ, DiPietro LA. Inflammation and wound healing: the role of the macrophage. *Expert Rev Mol Med.* 2011;13:e23.
  - 22 Tracy LE, Minasian RA, Caterson EJ. Extracellular Matrix and Dermal Fibroblast Function in the Healing Wound. *Adv Wound Care (New Rochelle).* 2016;5(3):119-36.
  - 23 Vallée A, Lecarpentier Y. TGF- $\beta$  in fibrosis by acting as a conductor for contractile properties of myofibroblasts. *Cell Biosci.* 2019;9(1):98
  - 24 Gürsoy EN, Sener K, Kùlahci MB, Balabanli KB, Cevher ŞC. Modern Strategies in Wound Healing: The Rise of Bacterial Cellulose Dressings. *Adv Ther.* 2025:e00072.
  - 25 Yuan F, Chang S, Luo L, Li Y, Wang L, Song Y, Wang Y. Cxcl12 gene engineered endothelial progenitor cells further improve the functions of oligodendrocyte precursor cells. *Exp Cell Res.* 2018;367(2):222-31.